

# Morphologies of three-dimensional shear bands in granular media

S. Fazekas

*Theoretical Solid State Research Group, Budapest University of Technology and Economics, H-1111 Budapest, Hungary*

J. Török

*Dept. of Chemical Information Technology Budapest University of Technology and Economics, H-1111 Budapest, Hungary*

J. Kertész

*Department of Theoretical Physics, Budapest University of Technology and Economics, H-1111 Budapest, Hungary*

D. E. Wolf

*Department of Physics, University Duisburg-Essen, D-47048 Duisburg, Germany*

(Dated: April 25, 2005)

Using three-dimensional Distinct Element Method with spherical particles we simulated shear band formation of granular materials in axisymmetric triaxial shear test. The calculated three-dimensional shear band morphologies are in good agreement with those found experimentally. We observed spontaneous symmetry breaking strain localization provided it was allowed by the boundaries. If the symmetry was enforced, we found strain hardening. We discuss the formation mechanism of shear bands in the light of our observations and compare our results with high resolution NMR experiments.

PACS numbers: 45.70.Cc, 81.40.Jj

Keywords: granular compaction, stress-strain relation

The description of the rheological properties of dry granular media is a key question which controls the ability of mixing, storing, transporting, etc. these particulate systems. An interesting and sometimes annoying feature of these materials is the strain localization to a narrow domain (shear band) which appears almost always when a sample is subject to deformation. The morphology of these failure surfaces is far from being understood.

Two dimensional or boundary induced shear band shapes have a vast literature dating back for decades including numerical and experimental studies. Three-dimensional studies have a major drawback as it is difficult to get information from inside the sample. In the past 10 years it gained increasing attention as experimental tools as Computer Tomography (CT) have became available[1, 2, 3]. Such studies revealed complex localization patterns and shear band morphologies depending on the test conditions.

In the engineering literature, large number of *constitutive models* of soils have been developed to describe granular experiments, however, it is recognized that many times it is difficult to relate the model parameters to soil properties and often their predictive power is restricted to one specific phenomenon [4]. Finite Element Method (FEM) commonly used in simulations of soils, is a good alternative of continuum based analysis. However they still require macroscopic *constitutive models* [5]. Recently, a simple theory based on the minimal dissipation principle was proposed and successfully used in a special configuration[6].

A different approach is the Distinct Element Method

[7] (also known as Molecular Dynamics) which simulates the individual grains of the sample based on microscopic contact model [8, 9]. Its drawbacks are the large computation need, especially in three dimensions, and limitations on the number and shape of the particles. However, as it is shown in this paper the computers of today are powerful enough that one can simulate realistic three-dimensional samples and obtain results that are in good agreement with the experiments. Furthermore, we hope that the complete knowledge of the inner state of the sample allows us to create more general models.

In this letter we report a distinct element (molecular dynamics) study of triaxial tests of cohesionless granular material. We show that depending on the boundary conditions different shear band morphologies can be observed similarly to experiments. We identify the shear bands by calculating the local shear intensity and show that it is correlated with the angular velocity of the particles and with the local void ratio and coordination number.

The most common axisymmetric triaxial test consists of a cylindrical specimen enclosed between two end platens and surrounded by a rubber membrane on which an external pressure is applied [1, 3]. The end platens are pressed against each other in a controlled way: Either with constant velocity (strain control) or with constant force (stress control). The force resulting on the platens, or the displacement rate of the platens is recorded, as well as the volume change of the specimen.

In our simulations presented here we used a standard DEM with Hertz contact model [10], appropriate damping [11], combined with a frictional spring-dashpot model

[8]. The technical details of the simulations (including the used parameter values) are presented elsewhere [12]. Here we summarize only the main points of the simulation setup.

The triaxial experiments are performed on vertical cylindrical samples of diameter  $D$  and height  $H \simeq 2D$  similarly to most experiments. This initial configuration was generated by the following method: The spherical grains with narrow Gaussian size distribution were randomly placed in a much taller ( $h = 3H$ ) solid cylinder which had the same width ( $D$ ). Apart from the size the grains had the same physical properties. After the placement the upper platen and the particles were given downwards velocities  $v = v_0 z/h$ , where  $z$  is the vertical coordinate of the object measured from the bottom platen which was fixed. The compressing force on the upper platen was switched on when the inner pressure of the particles could compensate for it. This choice of generating the initial condition was made because it is known to produce a homogeneous system and the initial void ratio of the system can be varied by changing the frictional coefficient during the preparation phase. However, in this letter we report simulations only where the particles were frictionless during the preparation thus the triaxial test were performed on dense systems. This preparational phase and the test were done in zero gravity.

During the testing the bottom platen was fixed. On the upper platen an axial load was applied and in certain tests it could rotate along the horizontal axes. In all tests presented here the friction coefficient of the particles was set to  $\mu = 0.5$ . The solid cylinder of the preparation was replaced by a cylindrical “elastic membrane” composed of overlapping spheres having equal diameter and mass density, and initially forming a triangular lattice on the superficies of the cylinder. The “membrane nodes” could not rotate and they were interconnected with linear springs having an elongation equal at any time to the relative distance of the nodes. The stiffness of the springs was chosen such that the particles could not escape by passing through the membrane. Additionally a homogeneous confining pressure  $\sigma_c$  was applied on the membrane which acted on the triangular facets formed by neighboring “membrane nodes”.

After the preparation phase, the sample was compressed by moving the upper platen downwards in vertical direction with a constant velocity (strain control). Starting from the same initial condition, we executed four different runs denoted by (A), (B), (C), and (D). We used two different compression velocities: a base value (A, B) and a two times larger value (C, D), and during compression, tilting of the upper platen was either enabled (A, C) or disabled (B, D).

During the compression we measured the local shear intensity ( $S$ ) generalizing the two-dimensional model of [13]. The regular triangulation [14] of the particle system is calculated [15], and for each particle the inci-

dent triangulation cells (tetrahedrons), and thus the discrete particle neighborhoods are identified. (The particles at the boundary, having infinite incident cells, are skipped.) Considering the piecewise linear interpolation  $\mathbf{u}$  of the particle displacements known from the DEM simulation over the regular triangulation, in a neighborhood  $\Omega$  of volume  $V$ , the components of the mean deformation gradient tensor can be calculated. Using the Gauss-Ostrogradski theorem the volume integral can be transformed into a closed surface integral over the  $\partial\Omega$  boundary of  $\Omega$ , leading to

$$\langle u_{ij} \rangle = \frac{1}{V} \oint_{\partial\Omega} n_i u_j dS, \quad (1)$$

where  $\mathbf{n}$  is the exterior normal along the boundary. Applying the above formula to discrete particle neighborhoods, the integration can be transformed into a summation over triangular facets, which is easy to implement.

Using the eigenvalues  $\varepsilon_k$  of the symmetric part of the local deformation gradient tensor, we define the local shear intensity as

$$S = \max_k \left| \varepsilon_k - \frac{1}{3} \sum_l \varepsilon_l \right|. \quad (2)$$

Consequently, taking vertical cross sections of the sheared samples and coloring the grains according to the local shear intensity ( $S$ ) we could identify shear bands Fig. 1 c,d) which clearly coincides with the change of velocity Fig. 1 a,b). According to our results when tilting of the upper platen is enabled, internal instabilities can develop into a localized deformation along a failure plane Fig. 1 c,e,f,g), while non-tilting platens act as a stabilizing factor leading to an axisymmetric hourglass shaped shear band with two conical surfaces Fig. 1 d,h,i,j). The latter case is also compared to experiments done in zero gravity and with non-tilting upper platen [3]. The nice correspondence of the form of the shear band as well as the nontrivial structure around it can be identified in spite of the rather limited size of our simulation. We measured the width of the shear bands to be  $\sim 12$  particle diameter which is about third of the width of the sample. We can conclude that in the absence of enforced axisymmetry, spontaneous symmetry breaking can take place [1, 2].

The simulation allows us to make the two different experiments (with or without tilting of the upper platen) on the *same* initial configuration and compare the resulting deformation field. The first significant non-axisymmetric difference appears as early as 2% of axial strain which is further enhanced in the non-axisymmetric case to an asymmetric shear plane and erased in the axisymmetric case. We also note that in the case with tilting upper platen the shear bands are not totally plane as can be seen on Fig. 1 e,f,g) but curved as the nearby boundary.

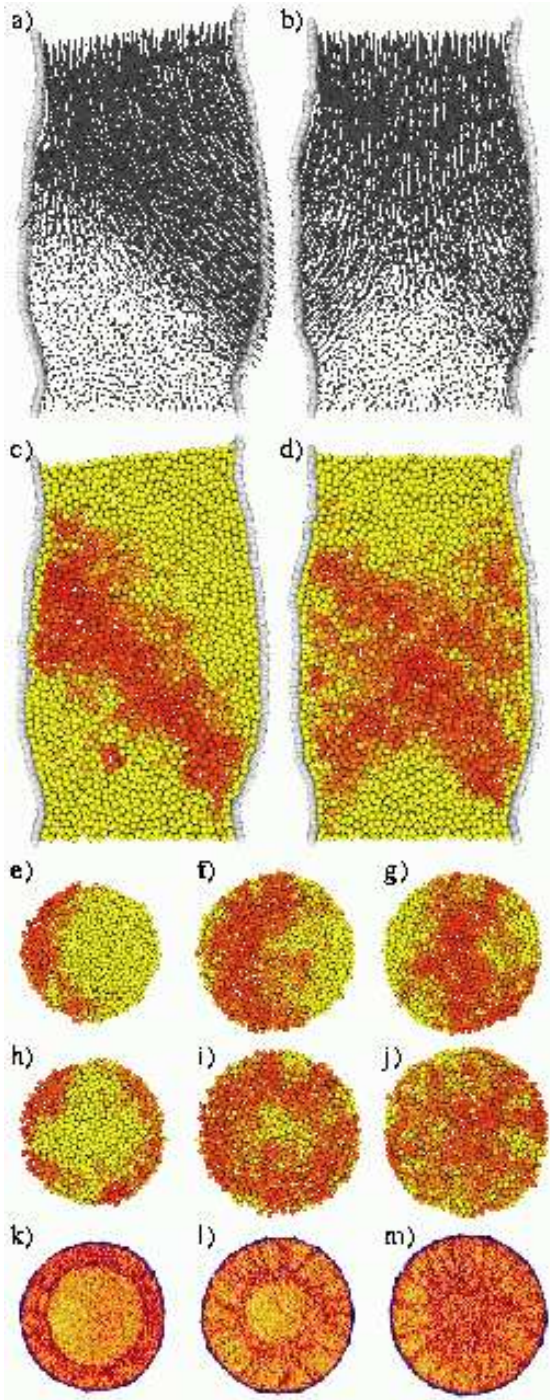


FIG. 1: Cross sections of samples are shown at 10% axial strain of sample (C) figs. a,c,e,f,g); of sample (D) figs. b,d,h,i,j); from [3] (F2075) figs. k,l,m). On figs. a,b) the velocity field of a vertical cut of the middle of the sample is shown, on figs. c,d) vertical, on figs. e-j) horizontal cross-sections are shown. The cuts were made at different height: close to the platen (e,h,k), in the middle of the sample (g,j,m) and in between (f,i,l). The red content of figs. e-j) is proportional to the local shear intensity on figs. k-l) to the local void ratio.

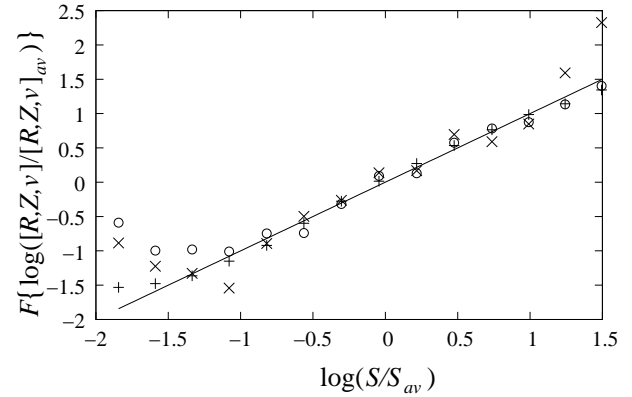


FIG. 2: Correlation of the local shear intensity and the angular velocity of grains (+), with  $F = x - 0.3$ , the coordination number ( $\times$ ), with  $F = 9(-0.27 - x)$ , the local void ratio ( $\circ$ ), with  $F = 27(x - 0.175)$ . The data is an average of all four runs at 10% axial strain.

This may only be a boundary effect but our sample is not big enough to answer this question.

In experiments like Computer Tomography the local void ratio is measured. On Fig. 1 we see nice correspondance between the measured local void ratio and our calculated local shear intensity. So we also measured the local void ratio, which is a macroscopic quantity and some average over a macroscopic volume is needed. If the cells chosen are very small we expect too large fluctuations. The smallest possible choice of elementary cells are the Voronoi cells of the particles. The void ratio in these cells is denoted by  $v$ . A good alternative to the local void ratio is (for nearly equal size spheres) the coordination number ( $Z$ ) which decreases as the local void ratio increases. Let us note that if the size distribution is wide enough a non-trivial particle size scaling of  $Z$  has to be taken into account.

In two dimensional systems the most common method for identifying the shear deformation is the rotation of the particles [16, 17] so we also measure the angular velocity of the particles and denote it by  $R$ .

All the four ( $S, R, Z, v$ ) quantities are defined for each particle thus we can easily check their correlation. We did a logarithmic binning (corresponding to the histogram) for the local shear intensity ( $S$ ) and averaged the other three quantities for the particles in the same bin. On Fig. 2 we compare the resulting values. The  $F$  function comes from a linear fit different for each data-set. The shift is a base value while the tilt shows the sensitivity of these quantities with respect to the local shear intensity. It was found to be 1 for the angular velocity, 9 for the coordination number and 27 for the local void ratio. The standard deviation was found to be proportional to the square root of the tilt. This means that the angular velocity is an essentially equivalent representation of the local shear intensity but the coordination number and

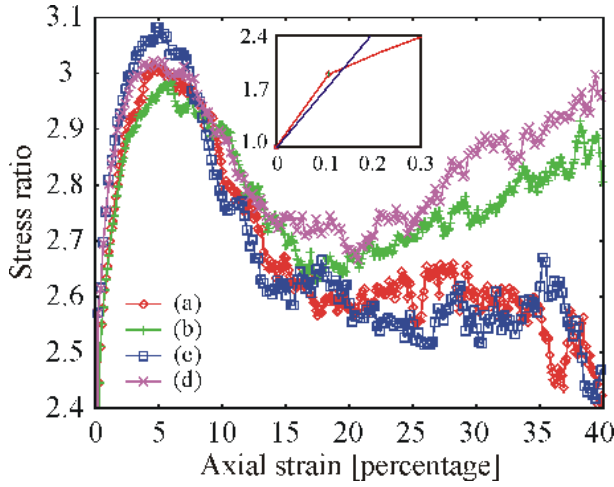


FIG. 3: (Color online) Stress-strain relation. The stress ratio  $\sigma/\sigma_0$  (where  $\sigma_0$  denotes the initial stress) measured on the upper platen is shown as function of the axial strain, for different simulation runs. (See inset for low strains.) For the lower two curves (A, C) tilting of the upper platen was enabled, and for the upper two (B, D) it was disabled.

the local void ratio are less sensitive thus they need more spatial and/or temporal averages to achieve the same accuracy in characterizing the shear intensity.

In order to compare to most common experiments, we measured the stress  $\sigma$  on the upper platen, and calculated the stress ratio  $\sigma/\sigma_0$  during the runs, where  $\sigma_0$  denotes the initial stress. As the axial strain increases, the response of the granular sample (the stress ratio) increases until it reaches a peak value, then decreases (see Fig. 3). According to Fig. 3, up to 15% axial strain there is no significant difference in the stress-strain relation measured in the different simulation runs, indifferent of the strain rate and tilting of the upper platen. Strain-softening of dense granular specimens is a basic observation of triaxial shear tests [18]. Any local deformation due to shear is followed by a dilatation resulting in a decrease of the force bearing capacity of the material, which in turn intensifies the deformation.

After about 15% of axial strain the data depart from each other. The different shear band shapes are responsible for this difference. The hourglass shaped shear band does not allow a simple flow of materials along the failure lines but particles leave and enter the shear band. As the test sample is further compressed the sample gets wider and shorter and opposes more firmly the compression thus the stress increases. In the case where the upper platen could tilt the hourglass shear band shape is not stable but the upper part slips away to one direction creating a nearly planar shear band. The plane structure of the failure line allows for a long intermediate state with two block like parts slipping on each other with the same constant stress.

In summary, we executed triaxial shear test simu-

lations using DEM. Different shear band morphologies known from experiments could be reproduced. To our knowledge it is the first time that these localization patterns were reproduced in DEM simulations. We have shown that in triaxial shear tests in a spontaneous way symmetry breaking strain localizations can develop if the axial symmetry is not enforced by non-tilting platens. We found strong correlation among the local shear intensity, the angular velocity of the grains, the coordination number and the local void ratio however the latter two are found to have larger fluctuations. The agreement of our results with the experimental results is very good, even if the system size (number of particles) in our simulations is much smaller than in experiments.

#### Acknowledgments

This research was carried out within the framework of the “Center for Applied Mathematics and Computational Physics” of the BME, it was supported by BMBF, grant HUN 02/011, and Hungarian Grant OTKA T035028, F047259.

---

- [1] J. Desrues, R. Chambon, M. Mokni, and F. Mazerolle, *Géotechnique* **46**, 529 (1996).
- [2] J. Desrues, in *X-ray CT for Geomaterials*, edited by J. Otani and Y. Obara (Balkema, 2004), pp. 15–41.
- [3] S. N. Batiste, K. A. Alshibli, S. Sture, and M. Lankton, *Geotechnical Testing Journal* **27**, 568 (2004).
- [4] D. M. Wood, *Soil Behaviour and Critical State Soil Mechanics* (Cambridge University Press, New York, 1990).
- [5] J. Tejchman and E. Bauer, *Gran. Mat.* **5**, 201 (2004).
- [6] T. Unger, J. Török, J. Kertész, and D. E. Wolf, *Phys. Rev. Lett.* **92**, 214301 (2004).
- [7] P. A. Cundall and O. D. L. Strack, *Geotechnique* **29**, 47 (1979).
- [8] S. Luding, in *The Physics of Granular Media*, edited by H. Hinrichsen and D. E. Wolf (Wiley-VCH, 2004).
- [9] T. Pöschel and T. Schwager, *Computational Granular Dynamics: Models and Algorithms* (Springer, Berlin, 2005).
- [10] L. D. Landau and E. M. Lifshitz, *Theory of Elasticity* (Pergamon, New York, 1970), chap. 9, (2nd English ed.).
- [11] N. V. Brilliantov, F. Spahn, J.-M. Hertzsch, and T. Pöschel, *Phys. Rev. E* **53**, 5382 (1996).
- [12] S. Fazekas, J. Török, J. Kertész, and D. E. Wolf, in *Powders and Grains 2005* (to be published, 2005).
- [13] D. Daudon, J. Lanier, and M. Jean, in *Powders and Grains 1997*, edited by Behringer and Jenkins (Balkema, 1997), pp. 219–222.
- [14] C. Lee, in *Applied Geometry and Discrete Mathematics: The Victor Klee Festschrift*, edited by P. Gritzmann and B. Sturmfels (American Mathematical Society, Providence, RI, 1991), pp. 443–456.
- [15] CGAL, <http://www.cgal.org>, Computational Geometry Algorithms Library (CGAL 2.4) (2003).
- [16] M. Oda and H. Kazama, *Geotechnique* **48**, 465 (1998).
- [17] H. J. Herrmann, J. A. Astrom, and R. M. Baram, *Physica A* **344**, 516 (2004).
- [18] P. V. Lade, *International Journal of Solids and Structures*

**39**, 3337 (2002).